Trajectory Planning for an Exoskeleton for Lower Limbs based on Torso Movements

Guilherme L. M. Silveira, s_guilherme_lm@hotmail.com
University of São Paulo at São Carlos, Mechanical Engineering Department, Mechatronics Laboratory, Av. Trabalhador São-carlense, 400 - São Carlos,SP, Brazil

Adriano A. G. Siqueira, siqueira@sc.usp.br
University of São Paulo at São Carlos, Mechanical Engineering Department, Mechatronics Laboratory

Abstract. *This paper presents a gait-pattern selection algorithm for exoskeletons based on the Zero Moment Point criterion. The proposed exoskeleton is developed for lower limbs and based on a commercially available orthosis. The step length and duration are considered as the selection parameters. First, these parameters are selected by the designer and a online controller based on the ZMP is implemented to generate stable trajectory for the exoskeleton. In the second strategy, the trajectory parameters are computed trough the torso movements generated by the patient intention of changing the gait-pattern. To test this selection method, it is proposed the principle of co-simulation where the degree of freedom of interest (hip) is replaced by a real motor. In this case, it is possible to apply real disturbances and make real measurements of the user intention.*

Keywords: *Exoskeleton, stable gait-pattern, ZMP, co-simulation*

1. INTRODUCTION

The use of robotic devices to allow intelligent aid of disabled and elderly people is increasing every year. Among the most promising of these devices are exoskeletons for lower limbs, which help the users giving them support, protection and necessary forces for a continuous walking (Guizzo & Goldstein 2005). Major advances in this area result from studies with biped robots. However, few rehabilitation devices proposed for patients with total or partial paralysis of lower limbs give the user the desired autonomy and safety (Ferris, Sawicki & Domingo 2005).

This work presents a control strategy to generate joint trajectories for an exoskeleton for lower limbs, considering the information obtained from sensors located in the hip. To make it possible, a trajectory generator based on the Zero Moment Point (ZMP) criterion is developed (Huang, Yokoi, Kajita, Kaneko, Arai, Koyachi & Tanie 2001). The ZMP is the point around which the sum of all moments of active forces is zero. It is described a method of optimization of the joint trajectories where the ZMP criterion is performed and a complete analysis of its convergence. The cubic spline interpolation method, where key points from the analysis of bipedal walking pattern, is used to generate the trajectories to be optimized. The position of the key points can be changed to adjust the speed or the gait pattern according to the user intention. The resulting trajectory can be analyzed through the simulation of a seven degrees of freedom model of the exoskeleton (Winter & Siqueira 2008).

Seeking to interpret the user intention and generate a trajectory compatible with it, a control strategy to select the parameters of the trajectory from the measurements obtained from the torso movements is developed. To test this selection method, it is proposed the principle of co-simulation where the degree of freedom of interest (hip) is replaced by a real motor. In this case, it is possible to apply real disturbances and make real measurements of the user intention. The desired torso trajectory is sent to the motor position controller, a hardware interface, and the actual joint torque, obtained from the motor current, is used as input to the trajectory selection strategy. According to the current value, the parameters of the trajectory optimization is increased or decreased by a given increment, generating a faster or slower gait-pattern, respectively.

The paper is organized as follows: Section 2.presents the trajectory generator for biped robots with some issues related to the optimization procedure; Section 3.introduces the control environment for exoskeleton for lower limbs and the result of the online control on the ZMP; Section 4.presents the gait-pattern selection algorithm based on the torque applied by the patient and the results obtained from the proposed strategy; and Section 5. summarizes the main contributions of the paper.

2. TRAJECTORY GENERATION WITH ZMP CRITERION

In this section, the trajectory generator for biped robots proposed in (Huang et al. 2001) is presented, with some considerations about the ZMP trajectory optimization. It is considered the exoskeleton is a biped robot with trunk, knees and feet, as shown in Figure 1. According to (Huang et al. 2001), the walking cycle can be divided in two phases, double support and single support. The double support phase starts when the heel of the forward foot touches the ground and finishes when the toe of the backward foot leaves the ground. The second phase is characterized by the fact only one foot

is in contact with the ground. In this work, the double support represents 20% of the entire walking cycle.

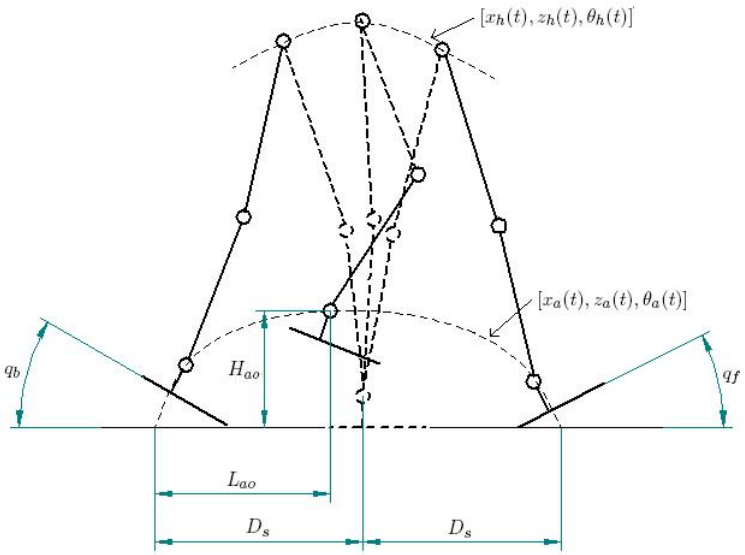

Figure 1. Biped robot model.

The foot and hip trajectories can be respectively parametrized as $X_a = [x_a(t), z_a(t), \theta_a(t)]^T$, where $(x_a(t), z_a(t))$ is the ankle position and $\theta_a(t)$ is the angle between the foot and the horizontal plane, and $X_h = [x_h(t), z_h(t), \theta_h(t)]^T$, where $(x_h(t), z_h(t))$ is the hip position and $\theta_h(t)$ is the angle between the trunk and the horizontal plane.

2.1 Foot trajectory

The step k occurs between the kT_c and $(k+1)T_c$ time instants, where T_c is the step time interval. Step k is defined starting when the heel of any foot leaves the ground and finishing when the same heel touches the ground again, Figure 2. q_b and q_f are the angles of the foot with relation to the horizontal at the initial and final time instants of the swing phase (single support), respectively.

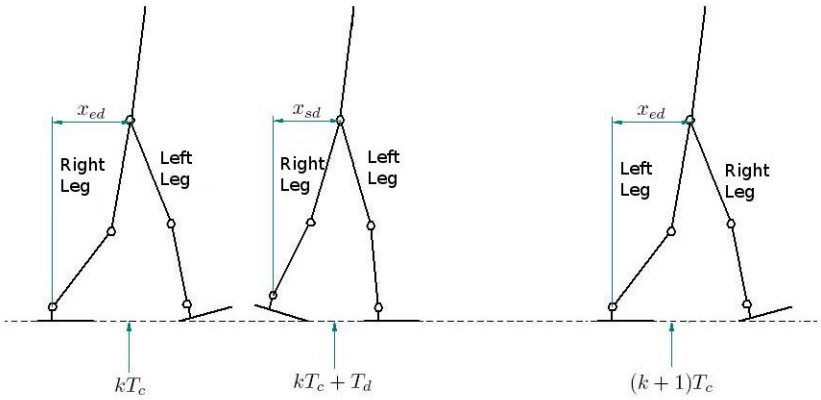

Figure 2. Walking cycle, double and single support phases.

Assuming that the left foot is completely in contact with the ground during the times $kT_c + T_d$ and $(k+1)T_c$, the following conditions can be stated:

$$\theta_a = \begin{cases} q_{gs}(k), & t = kT_c \\ q_b, & t = kT_c + T_d \\ -q_f, & t = (k+1)T_c \\ -q_{ge}(k), & t = (k+1)T_c + T_d \end{cases} \tag{1}$$

where T_d is the time interval of the double support phase, $q_{gs}(k)$ and $q_{ge}(k)$ are the ground slope for the initial and final step instants, respectively.

The following specifications can also be defined for the foot position:

$$x_a = \begin{cases} kD_s, & t = kT_c \\ kD_s + l_{an}sin(q_b) & \\ \quad +l_{af}(1-cos(q_b)), & t = kT_c + T_d \\ kD_s + L_{ao}, & t = kT_c + T_m \\ (k+2)D_s - l_{an}sin(q_f) & \\ \quad -l_{ab}(1-cos(q_f)), & t = (k+1)T_c \\ (k+2)D_s, & t = (k+1)T_c + T_d \end{cases} \qquad z_a = \begin{cases} h_{gs}(k) + l_{an}, & t = kT_c \\ h_{gs} + l_{af}sin(q_b) + l_{an}cos(q_b), & t = kT_c + T_d \\ H_{ao}, & t = kT_c + T_m \\ h_{ge} + l_{ab}sin(q_f) + l_{an}cos(q_f), & t = (k+1)T_c \\ h_{ge}(k) + l_{an}, & t = (k+1)T_c + T_d \end{cases} \tag{2}$$

where (L_{ao}, H_{ao}) is the higher foot position (this position occurs at $kT_c + T_m$), D_s is the step length, l_{an} is the foot height and l_{af} is the distance between the heel and the ankle joint. The heights of the ground when the foot is touching it are defined as $h_{gs}(k)$ and $h_{ge}(k)$, for the initial and final step instants, respectively. Some constraints on right foot velocities are also imposed, see (Huang et al. 2001) details. A smooth trajectory can be generated through the interpolation method based on cubic splines, where second order differentiable trajectories are generated for all time interval.

2.2 Hip trajectory

It is considered that the angle between the trunk and the horizontal axis $\theta_h(t)$ presents no variation along the walking cycle. Also, as the position of the ZMP is not affected by the hip motion in the z direction, it is assumed a little variation between the highest position H_{hmax} and the lowest position H_{hmin}, where the former occurs at the middle of the single support phase and the second at the middle of the double support phase. That is, z_h can be defined as:

$$z_h = \begin{cases} H_{hmin}, & t = kT_c + 0,5T_d \\ H_{hmax}, & t = kT_c + 0,5(T_c - T_d) \\ H_{hmin}, & t = (k+1)T_c + 0,5T_d. \end{cases} \tag{3}$$

Considering the sagittal plane, the hip motion along the x direction is the main contribution for the ZMP be inside the support polygon. In (Huang et al. 2001) it is proposed generate a set of stable trajectories $x_h(t)$ and select the trajectory with large stability margin according to the ZMP criterion.

The following conditions are defined for the hip trajectory along the x direction:

$$x_h = \begin{cases} kD_s + x_{ed}, & t = kT_c \\ (k+1)D_s - x_{sd}, & t = kT_c + T_d \\ (k+1)D_s + x_{ed}, & t = (k+1)T_c \end{cases} \tag{4}$$

where x_{sd} and x_{ed} are the distances along the x direction from the hip to the ankle of the support foot at the initial and final time instants of the swing phase, respectively. In this paper, these values are constrained to $x_{sd} \in (0; 0.5D_s)$ and $x_{ed} \in (0; 0.5D_s)$.

Considering the interpolation method based on cubic splines, it is possible to generate different trajectories and to select the best one according to the ZMP criteria. To guarantee that the ZMP remains most of the time next to the center to the support polygon, the following functional is defined:

$$J(x_{ed}, x_{sd}) = \frac{\sum_{n=1}^{p} d_{ZMP}^2}{p}, \tag{5}$$

where d_{ZMP} is the distance between the ZMP and the center of the stability region defined by the convex polygon of the contact points and p is the number of points throughout the trajectory in which d_{ZMP} is computed.

2.3 Optimization issues

The steepest descent algorithm was selected as the optimization method. It presents an easy implementation and high convergence rate after all parameters be adjusted. The computation of J is highly time consuming if a representative number of trajectory points p must be considered. The algorithm is defined as:

$$\overline{X}_{n+1} = \overline{X}_n - \eta \nabla J(x_{ed}, x_{sd}) \tag{6}$$

where $\overline{X}_n$ is the vector containing the values of x_{ed} and x_{sd} for optimization step n, η is the optimization rate and $\nabla J(x_{ed}, x_{sd})$ is the functional gradient with relation to x_{ed} and x_{sd}.

As shown in Section 2. the minimization of J is constrained to $x_{sd} \in (0; 0.5D_s)$ and $x_{ed} \in (0; 0.5D_s)$. Hence, it is necessary to constrain the algorithm to these values. Also, there are values of x_{ed} and x_{sd} for which there is no solution for the inverse kinematic used to compute the shin and thigh absolute angles. The functional J is defined constant and

equal to zero in this region. If the result from optimization, $\overline{X}_{n+1}$, is outside the functional domain (where J is imposed to be zero), the optimization stops, because $\nabla J(x_{ed}, x_{sd}) = 0$. $\nabla J(x_{ed}, x_{sd})$ is computed numerically by a small variation on the parameters. According to the selected initial condition, the above problem occurs frequently if the optimization rate is not properly selected.

The following strategy was defined to solve this problem: if the optimization result belongs to the area outside the functional domain ($J = 0$ and $\nabla J = 0$), it is defined a convergence direction perpendicular to the last $\nabla J \neq 0$, until the result belongs to the domain. Figure 3 shows a minimization results where the proposed strategy is utilized and the final result is inside the functional domain.

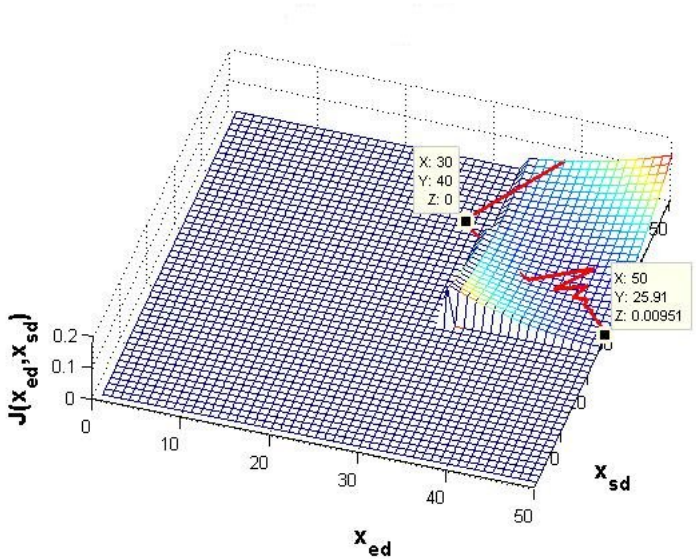

Figure 3. Optimization results for initial value $\overline{X}_0 = [0.3\ 0.4]^T$ and optimal value $\overline{X}_{opt} = [0.5\ 0.26]^T$. The proposed strategy for points outside the functional domain is used at the second optimization step.

Figure 4 shows the surfaces of J for different values of D_s and T_c. This analysis is important because D_S and T_c define a essential characteristic of the gait-pattern, the velocity. By changing these parameters, a wide variation of trajectories can be created.

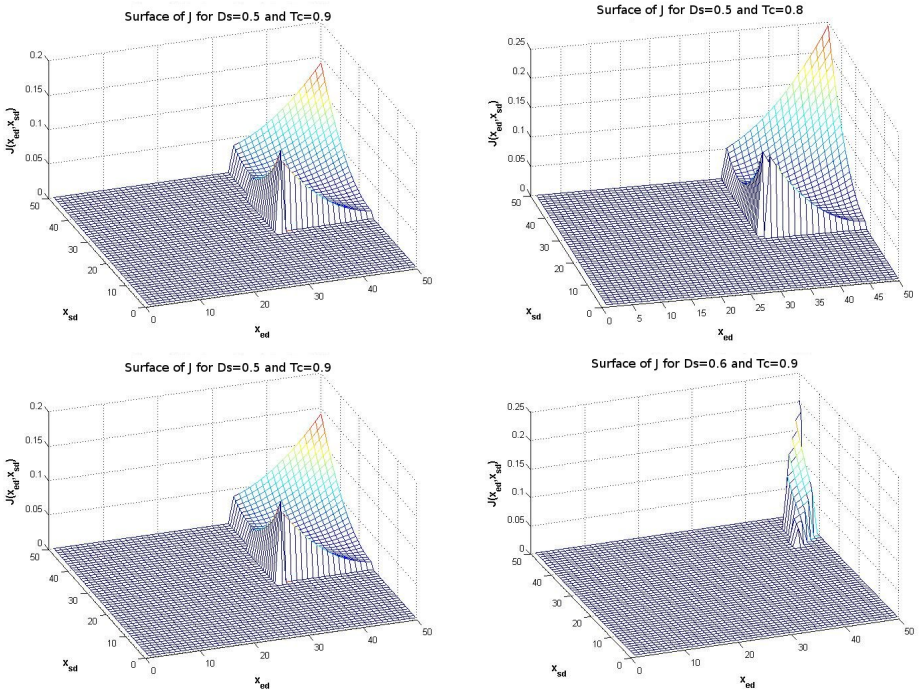

Figure 4. Surfaces of J for different values of D_s and T_c.

It can be noted from Figure 4 that the variation of T_c does not affect the surface of J. However, for a little variation on D_s the domain of J is extremely reduced. In this case, there is no solution for the inverse kinematic for a wide range of values. That is, there are few trajectories which maintain the hip height and develop a large step length, $D_s = 0.6$ m.

From the analysis of the variation of J given a variation of D_s, it is proposed a relation between the step length, D_s, and the maximum height, H_{hmax}. For a given D_s, H_{hmax} can be computed as the height of the isosceles triangle defined by base Ds and sides $L_{th} + L_{sh}$ plus the ankle height. This value is parametrized by parameters defined as function of $(Ds - 0.5)$ an $(Tc - 0.9)$, the differences from the initial values of D_s and T_c, as shown in the following equations:

$$H_{hmax} = \left(\sqrt{(L_{sh} + L_{th})^2 - (\frac{D_s}{2})^2} + l_{an} \right) .\alpha_1 .\alpha_2, \tag{7}$$

$$\begin{cases} \alpha_1 = \left(\frac{D_s - 0.5}{0.5}\right)^2 - 1, & D_s - 0.5 > 0, \\ \alpha_1 = 1, & D_s - 0.5 < 0, \end{cases} \qquad \alpha_2 = \left(\frac{|T_c - 0.9|}{0.9} \right)^{3.2} - 1. \tag{8}$$

where L_{sh} and L_{th} are the lengths of the shin and thigh, respectively.

Figure 5 shows the surfaces for J computed for different values of D_S and considering the empirical relation for H_{hmax}. Note that the functional domain remains suitable for the optimization, even with the variation of D_s.

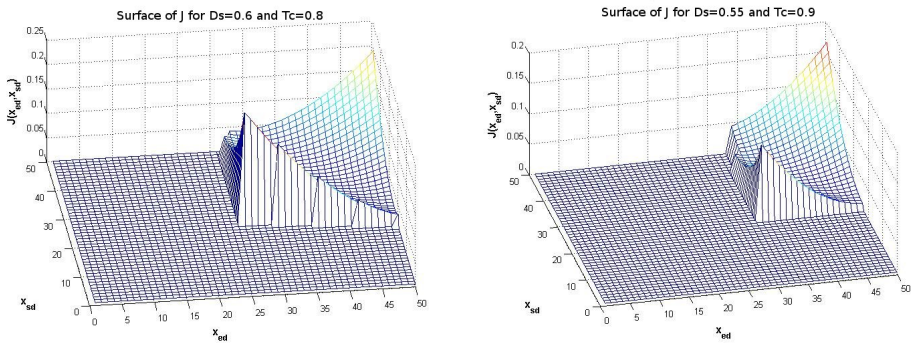

Figure 5. Surfaces for J considering the empiric relation for H_{hmax}.

3. EXOSKELETON CONTROL ENVIRONMENT

This section presents the exoskeleton dynamic parameters, a brief description of the control environment where the trajectory generator is implemented and the resuts of the first control strategy, based on the online control of the ZMP. The orthosis used for the exoskeleton for lower limbs corresponds to one Reciprocating Gait Orthosis LSU (Lousiana State University). Figure 6 shows the orthosis and the exoskeleton design, created in the Solid Egde software. It is considered that all joints in the sagittal plane will be driven by an Series Elastic Actuator (SEA). SEA can performed force and impedance controls, which can be used to generate a variable impedance controller (Walsh, Paluska, Pasch, Grand, Valiente & Herr 2006).

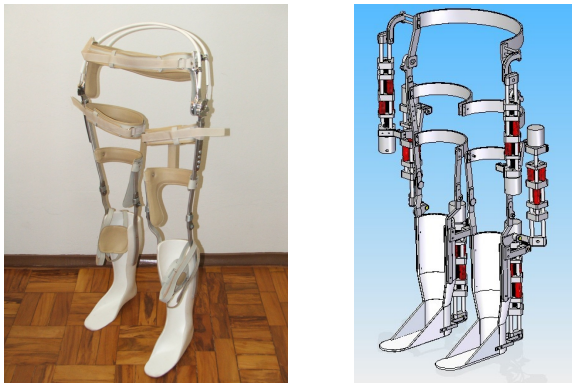

Figure 6. RGO orthosis and exoskeleton design (Solid Edge).

The dynamic parameters of the orthosis, shown in Tab. 1, was obtained by the Solid Edge model. It is also presented the parameters of the patient considered in the simulation, obtained from (Winter 1990), considering a 85 kg, 1.74 m individual.

Table 1. Orthosis and Patient Dynamic Parameters.

Orthosis		**Patient**	
$M_{total,ort}$	4.8	$M_{total,pat}$	85
$L_{total,ort}$	1.0	$L_{total,pat}$	1.74
Limb Mass (kg)			
$M_{tigh,ort}$ 0.95		$M_{tigh,pat}$	8.5
$M_{leg+foot,ort}$	0.72	$M_{leg+foot,pat}$	5.2
$M_{torso,ort}$	1.49	$M_{torso,pat}$	57.6
Limb Length (m) - z direction			
$L_{tigh,ort}$	0.39	$L_{tigh,pat}$	0.39
$L_{leg+foot,ort}$	0.49	$L_{leg+foot,pat}$	0.49
$L_{torso,ort}$	0.12	$L_{torso,pat}$	0.87

An analytical model of the orthosis ground reaction forces, is developed using the Symbolic Toolbox of the Matlab. Figure 7 shows the motion animation of the orthosis-patient system for a simulation of two steps. In the initial step it is considered $D_s = 0.45$ and $T_c = 0.9$. For the second step $D_s = 0.58$ and $T_c = 0.8$. Only the orthosis representation is shown since the patient dynamic is incorporated in the orthosis dynamics.

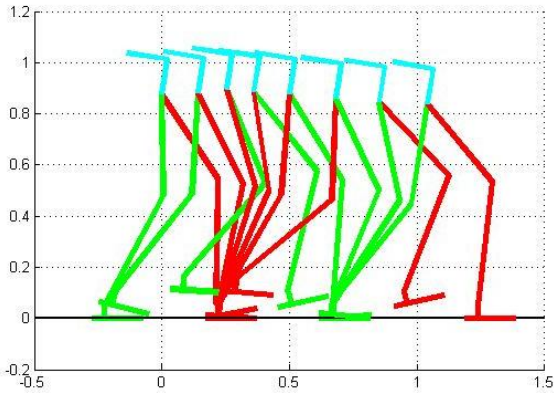

Figure 7. Motion animation of the orthosis-patient system.

It can be observed that the algorithm obtained satisfactory results with relation to the selection of the parameters used to generate trajectory desired by patient.

3.1 Orthosis-patient dynamics

To implement the gait-pattern selection algorithm, the orthosis is modeled according to the basic robotic equation,

$$M_{ort}(q)\ddot{q} + C_{ort}(q,\dot{q}) + G_{ort}(q) = \tau_a + \tau_{pat} + \tau_d, \tag{9}$$

where $q \in \Re^n$ is the generalized coordinates vector, $M \in \Re^{nxn}$ is the symmetrical, positive definite inertia matrix, $C \in \Re n$ is the centrifugal and Coriolis torques vector, and $G \in \Re^n$ is the gravitational torques vector. The terms $\tau \in \Re^n$ are the torques acting in orthosis: τ_a is the torque supplied by the actuators, τ_{pat} is the torque generated for the orthosis-patient interaction, and τ_d is the torque generated by any external disturbances acting in the patient-orthosis system.

The torque of interaction between the orthosis and the patient, τ_{pat}, can be divided in active and passive components. The passive patient torque, $\tau_{pat,pas}$, is the torque necessary to move the patient if he/she is moving in a passive way. In case that the patient influences in the orthosis movement, he/she will produce the active patient torque, $\tau_{pat,at}$. Therefore, Eq. (9) can be rewrite, considering now, the orthosis-patient dynamics,

$$M_{ort+pat}(q)\ddot{q} + C_{ort+pat}(q,\dot{q}) + G_{ort+pat}(q) = \tau_a + \tau_{pat,act} + \tau_d, \tag{10}$$

where $M_{ort+pat}(q)$, $C_{ort+pat}(q,\dot{q})$, and $G_{ort+pat}(q)$ correspond to the combination of the orthosis and patient dynamics.

The following results show the position of the ZMP for a given stable trajectory, Fig. 8. They were obtained using the simulator and considering the position control strategy proposed in (Gomes, Silveira & Siqueira 2009). In the graphics

containing ZMP measurements, the origin of the coordinate system is transferred to zero when one foot touch the ground and the other leaves.

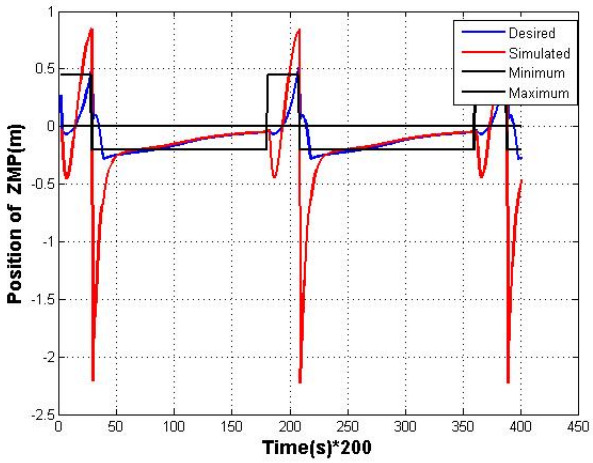

Figure 8. ZMP position, off-line control strategy.

As one can note, the desired trajectory of the ZMP, which was optimized using the procedure described above, is most of the time within the stable region. However, the simulated trajectory, even disregarding the negative peak, generated because of the way in which the forces of contact are computed, becomes outside the stable region for a long period of time and further from its center. To correct this deviation from the desired trajectory, we suggest the application of an on-line control based on the ZMP.

3.2 Online control based on the ZMP

The proposed controller to improve the position of ZMP is a PD one,

$$\tau_{\theta_4} = K_p d_{zmp} + K_d \dot{d}_{zmp}, \tag{11}$$

where K_p and K_d are gains selected by the designer. It is applied to the joint between the torso and thigh of the support leg and is computed with relation to the center of the stable region. This angle directly influences the position of the leg and torso in balance, thus significantly changes the position of ZMP. But, as the simple and double support dynamics are different, the control parameters are different in each stage. Figure 9 shows the results of the proposed control strategy.

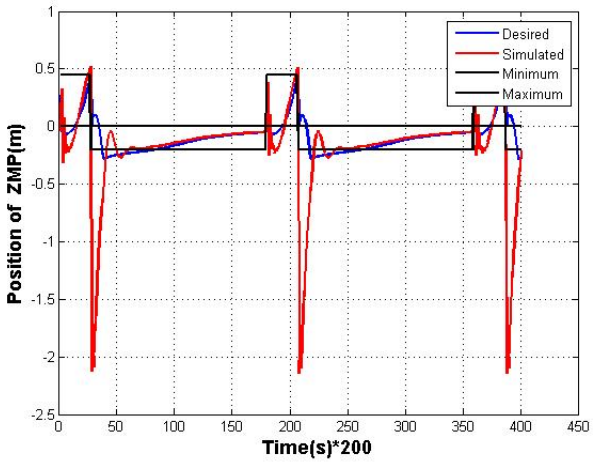

Figure 9. ZMP position, online control strategy.

It can be concluded that the online control strategy is effective to bring the ZMP to the center of the stable region in the double support phase, and make it returns to the region of stability faster, during the single support phase. Therefore, this control is effective in improving the overall stability of the system. The same control strategy can be applied considering the ankle joint as actuation point. This actuation changes directly the ground reaction forces and the position of the waist, thus changing the position of ZMP. The results are similar to the previous one.

4. CO-SIMULATION

The second control strategy proposed in this paper is the selection of the desired trajectory from the torque applied by the patient trough his/her torso. It is defined a proportional relation between the speed of the step, which was previously described, and the torque applied by the patient. This user intention can be measured by reading the motor current. The following adaptation law is proposed,

$$\Delta V_{step} = \Delta\left(\frac{D_s}{T_c}\right) = K_\Delta . K_t . i_m, \tag{12}$$

where K_Δ is a gain selected by the designer, K_t is the motor torque constant and i_m is the motor current. To ensure this principle is suitable, the control environment was modified through the interpreted programming language in the MATLAB for compiled language using textit (mex) files, thus the simulator can make the integration in a time as closer as possible to real. To speed up the integration time, we also implement a fourth-order *Runge Kutta* integration method.

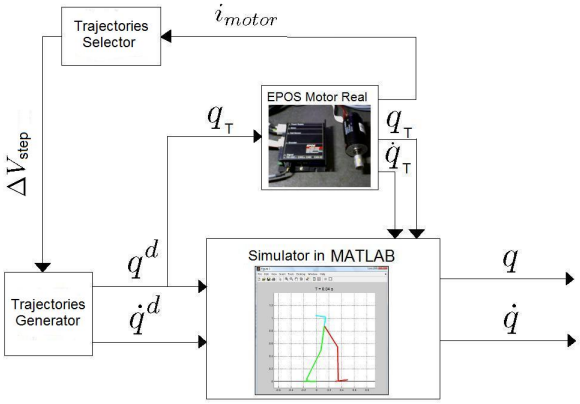

Figure 10. Co-simulation implementation setup.

With this assumptions, we can apply the concept of co-simulation, in which one of the seven degrees of freedom that define the system is replaced by a real motor. The motor position simulates the torso position of the patient. The implementation setup is composed by a DC motor (Maxon Motors), controlled by the digital positioning controller EPOS. This device implements a PID control to follow the desired position for this joint, generated by the trajectory planning. In the control environment , the response of the differential equation for this parameter is replaced by actual values measured by the motor encoder. Therefore, any disturbance applied to the motor changes the simulation. This concept can be better understood by the block diagram of Figure 10.

When the user intents to change the actual position of the motor, the internal control will increase the torque applied to maintain the desired position. This applied torque increase can be measured from the applied current to the motor.

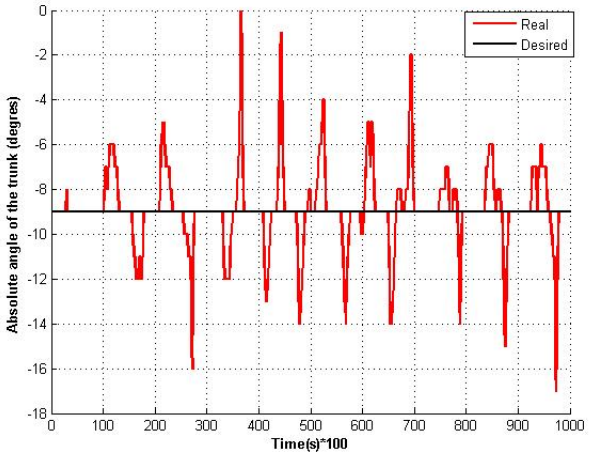

Figure 11. Desired and real torso trajectories.

Thus, during the step, the user can change the position of the motor according to the exoskeleton posture shown in the

control environment interface. It is necessary to exert an average torque during the step from which it can be defined the variation of the speed of the next desired step, Eq. 12. The results of one of these tests are shown in Figures 11 and 12.

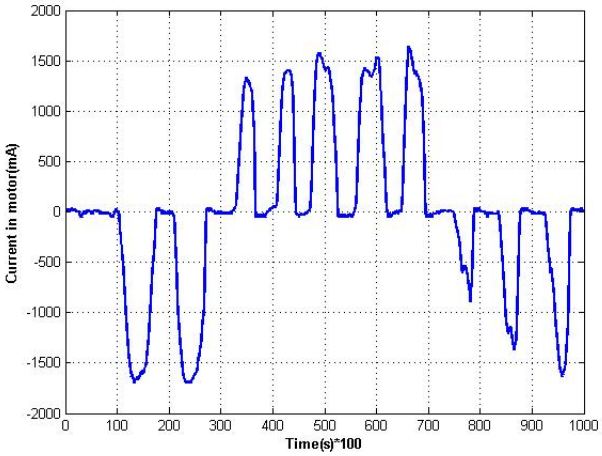

Figure 12. Applied current.

From the above graphs, it can be seen that if the user tries to give up the desired trajectory, the current supplied to the motor increases indicating that the patient is trying to move faster. The selection of trajectories using the current can be seen in Table 2, emphasizing that the average torque of a step changes the speed of the next step.

Table 2. Trajectory parameters for each step.

Step	1	2	3	4	5	6	7	8	9	10	11	12
$D_s\ (m)$	0.51	0.51	0.49	0.47	0.50	0.53	0.55	0.57	0.59	0.58	0.56	0.54
$T_c\ (s)$	0.9	0.9	0.9	0.9	0.9	0.9	0.9	0.9	0.9	0.9	0.9	0.9
$i_m\ (A)$	-7	-449	-455	516	652	401	395	391	-219	-395	-396	-

5. CONCLUSIONS

This paper deals with trajectory planning for an exoskeleton for lower limbs. It was observed the trajectory generator proposed in (Huang et al. 2001) and based on the ZMP criterion is suitable to perform adaptation algorithms for exoskeletons. First, it was observed that the imperfections of the trajectory of the ZMP can be corrected by a control based on the error of this position. It is also presented the implementation of a gait-pattern selection algorithm, which considers the orthosis-patient interaction through the analysis of the torso torque and the ZMP criterion, allowing the patient to modify the gait-pattern and still maintaining the walking stability. The simulation results show the proposed selection algorithms can be applied in the actual exoskeleton being constructed.

6. ACKNOWLEDGEMENTS

This work is supported by FAPESP(Fundação de Amparo à Pesquisa do Estado de São Paulo) under grants 2008/09530-4 and 2008/02317-8.

7. REFERENCES

Ferris, D. P., Sawicki, G. S. & Domingo, A. R. (2005). Powered lower limb orthoses for gait rehabilitation, *Top Signal Cord inj. Rehabilitation* **11**(2): 34–49.

Gomes, M. A., Silveira, G. L. M. & Siqueira, A. A. G. (2009). Towards gait-pattern adaptation algorithms for exoskeletons based on the zmp criterion, *Proceedings of the European Control Conference (ECC09)*, Budapest, Hungary.

Guizzo, E. & Goldstein, H. (2005). The rise of the body bots, *IEEE Spectrum (INT)* **42**(10): 42–48.

Huang, Q., Yokoi, K., Kajita, S., Kaneko, K., Arai, H., Koyachi, N. & Tanie, K. (2001). Planning walking patterns for a biped robot, *IEEE Transactions on Robotics and Automation* **17**(3).

Walsh, C. J., Paluska, D. J., Pasch, K., Grand, W., Valiente, A. & Herr, H. (2006). Development of a lightweight, underactuated exoskeleton for load-carrying augmentation, *Proceedings of the 2006 IEEE International Conference on Robotics and Automation*, Orlanda, Florida.

Winter, D. A. (1990). *Biomechanics and motor control of human gait*, 2 edn, John Wiley Interscience.
Winter, T. F. & Siqueira, A. A. G. (2008). Modelagem e simulação de um exoesqueleto para membros inferiores, *Anais do XVII Congresso Brasileiro de Automática, CBA2008*, Juiz de Fora, Brasil.

8. Responsibility notice

The author(s) is (are) the only responsible for the printed material included in this paper